Polym. Bull. (2009) 63:267–282
DOI 10.1007/s00289-009-0084-5

ORIGINAL PAPER

Non-isothermal degradation kinetics of poly (2,2′-dihydroxybiphenyl)

Fatih Doğan · İsmet Kaya · Ali Bilici

Received: 14 January 2009 / Revised: 28 March 2009 / Accepted: 14 April 2009 /
Published online: 29 April 2009
© Springer-Verlag 2009

Abstract Catalytic oxidative polymerization of 2,2′-dihydroxybiphenyl (DHBP) was performed by using Schiff base polymer-Cu (II) complex and hydrogen peroxide as catalyst and oxidant, respectively. According to size exclusion chromatography (SEC) analysis, the number-average molecular weight (M_n), weight-average molecular weight (M_w) and polydispersity index (PDI) values of poly (2,2′-dihydroxybiphenyl) (PDHBP) were found to be 37,500, 90,000 g mol^{-1} and 2.4, respectively. The thermal degradation kinetics was investigated by thermogravimetric analysis in dynamic nitrogen atmosphere at four different heating rates: 5, 10, 15 and 20 °C min^{-1}. The derivative thermogravimetry curves of PDHBP showed that its thermal degradation process had one weight-loss step. The apparent activation energies of thermal decomposition for PDHBP as determined by Tang, Flynn–Wall–Ozawa (FWO), Kissenger–Akahira–Sunose (KAS), Coats–Redfern (CR) and Invariant kinetic parameter (IKP) methods were 109.1, 109.0, 110.0, 108.4 and 109.8 kJ mol^{-1}, respectively. The mechanism function and pre-exponential factor were determined by master plots and Criado–Malek–Ortega method. The most likely decomposition process was a D_n Deceleration type in terms of the CR, master plots and Criado–Malek–Ortega results.

F. Doğan (✉)
Faculty of Education, Secondary Science and Mathematics Education,
Çanakkale Onsekiz Mart University, 17100 Çanakkale, Turkey
e-mail: fatihdogan@comu.edu.tr

İ. Kaya
Department of Chemistry, Faculty of Science and Arts,
Çanakkale Onsekiz Mart University, 17020 Çanakkale, Turkey

A. Bilici
Control Laboratory of Agricultural and Forestry Ministry, 17100 Çanakkale, Turkey

Keywords Poly (2,2′-dihydroxybiphenyl) · Kinetic parameter · Mechanism function

Introduction

The oxidative coupling polymerization of phenol derivatives constitutes a class of interesting research topic. Recently syntheses of polyphenols have received much attention due to their thermal and mechanical properties [1–5]. One of the syntheses methods of polyphenols is catalytic oxidative polymerization. Catalytic oxidative polymerization of phenols provides an environmentally benign method to synthesize phenol polymers [6]. Many catalytic systems have been employed to obtain these polymers such as enzymes, Schiff base-metal complexes as well as transition metal salts [7, 8].

These compounds have structures normally composed of a mixture of phenylene and oxyphenylene units, which are formed by C–C and C–O coupling of phenols. Poly (1,4-phenylene oxide) (PPO) is the representative polymer produce by the oxidative polymerization. PPO is widely used as a high-performance engineering plastic, since the polymer has excellent chemical and physical properties such as high glass transition temperature and mechanically tough property. In addition, blends of PPO are widely used as engineering plastics in industrial fields [9]. Therefore, oxidative polymerization of phenolic compounds has been extensively studied by many researchers. Kobayashi et al. examined the thermal properties of bisphenol polymers [10]. They have reported that polymers from dihydroxydiphenylmethanes showed relatively high thermal stability. Enzymatic oxidative polymerization of phenol was carried out by Oguchi et al. [11] and they reported that soluble polyphenol possessing high thermal stability.

The aim of the present work is to understand the decomposition mechanism of PDHBP which is a member of polyphenol family. The activation energies of thermal degradation of PDHBP in N_2 were obtained by Tang, KAS, FWO, CR and IKP methods. Thermal degradation mechanism for PDHBP was investigated by CR method, master plots method and Criado–Malek–Ortega method.

Experimental

Materials

DHBP and all solvents were supplied from Merck Chem. Co. (Germany). The synthesis PDHBP (Scheme 1) is given in detail under the sentence of poly-2-hydroxyphenyliminomethylphenol and poly-2-hydroxyphenyliminomethylphenol-Cu(II) complex compound prepared according to reported procedures [12–14].

Synthesis of poly-2-hydroxyphenyliminomethylphenol-Cu(II) complex

A solution of Cu $(AcO)_2$ $4H_2O$ (1 mmol) in methanol (10 ml) was added to a solution of poly-2-hydroxyphenyliminomethylphenol (1 mmol unit^{-1}) in tetrahydrofuran (20 mL). The mixture was stirred and heated at 70 °C for 5 h. The

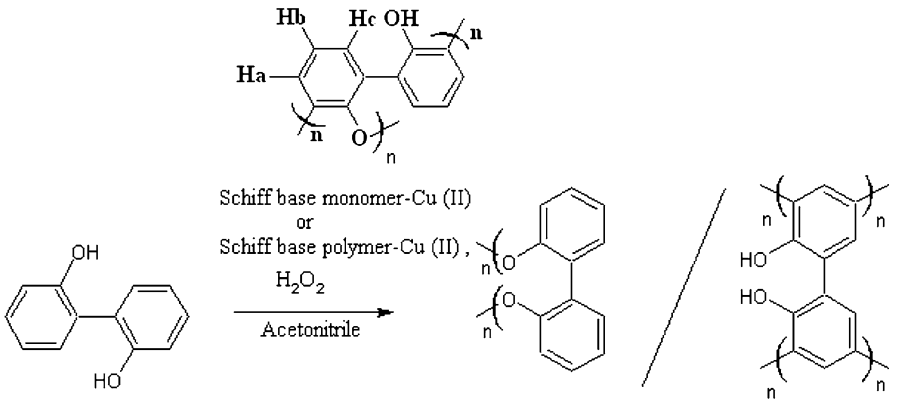

Scheme 1 Oxidative polymerization of DHBP

precipitated complex was filtered, washed with cold methanol/tetrahydrofuran (1:1) and then dried in vacuum oven.

Measurements

The number-average molecular weight (M_n), weight-average molecular weight (M_w) and polydispersity index (PDI) values of polymer were determined by size exclusion chromatography (SEC) (Shimadzu Co. Japan) with a Macherey-Nagel GmbH & Co. (Germany) (100 Å and 7 nm diameter loading material) 7.7 mm i.d. × 300 mm columns, DMF/MeOH eluent (0.4 mL min^{-1}, v/v, 4/1), polystyrene standards and a refractive index detector. Thermal data were obtained by using Perkin Elmer Diamond Thermal Analysis. The TG-DTA measurements were made between 15–1,000 °C (in N_2, heating rates 5, 10, 15 and 20 °C min^{-1}).

Kinetics methods

The application of dynamic TG methods holds great promise as a tool for unraveling the mechanisms of physical and chemical processes that occur during polymer degradation. In this paper, integral isoconversional methods were used to analyze the non-isothermal kinetics of PDHBP.

The rate of solid-state non-isothermal decomposition reactions is expressed as

$$\frac{d\alpha}{dT} = \left(\frac{A}{\beta}\right) \exp\left(\frac{-E}{RT}\right) f(\alpha). \tag{1}$$

Rearranging Eq. 1 and integrating both sides of the equation leads to the following expression

$$g(\alpha) = \left(\frac{A}{\beta}\right) \int_{T_0}^{T} \exp\left(\frac{-E}{RT}\right) dT = \left(\frac{AE}{\beta R}\right) p(u) \tag{2}$$

where $p(u) = \int_{\infty}^{u} -\left(\frac{e^{-u}}{u^2}\right)du$ and $u = E/RT$.

Flynn–Wall–Ozawa method [15, 16]

This method is derived from the integral method. The technique assumes that the A, $f(\alpha)$ and E are independent of T while A and E are independent of α, then Eq. 2 may be integrated to give the following in logarithmic form:

$$\log g(\alpha) = \log(AE/R) - \log \beta + \log p(E/RT). \tag{3}$$

Using Doyle's approximation [17] for the integral which allows for $E/RT > 20$, Eq. 3 now can be simplified as

$$\log \beta = \log(AE/R) - \log g(\alpha) - 2.315 - 0.4567\, E/RT. \tag{4}$$

Coats–Redfern method [18]

Coats–Redfern method is also an integral method, and it involves the thermal degradation mechanism. Using an asymptotic approximation for resolution of Eq. 2, the following equation can be obtained:

$$\ln\left(\frac{g(\alpha)}{T^2}\right) = \ln\left(\frac{AR}{E\beta}\right) - \frac{E}{RT}. \tag{5}$$

The expressions of $g(\alpha)$ for different mechanism have been listed Table 1 [19, 20], and activation energy for degradation mechanism can be obtained from the slope of a plot of ln $[g(\alpha)/T^2]$ versus $1{,}000/T$

Tang method [21]

Taking the logarithms of sides and using an approximation formula for resolution of Eq. 2, the following equation can be obtained:

$$\ln\left(\frac{\beta}{T^{1.894661}}\right) = \ln\left(\frac{AE}{R\,g(\alpha)}\right) + 3.635041 - 1.894661\ \ln E - \frac{1.001450E}{RT}. \tag{6}$$

The plots of $\ln\left(\frac{\beta}{T^{1.894661}}\right)$ versus $1/T$ give a group of straight lines. The activation energy E can be obtained from the slope $-1.001450\ E/R$ of the regression line.

Kissenger–Akahira–Sunose method [22]

This method is integral isoconversional methods as FWO.

$$\ln\left[\frac{\beta}{T^2}\right] = \ln\left[\frac{AR}{E\,g(\alpha)}\right] - \frac{E}{RT}. \tag{7}$$

The dependence of ln (β/T^2) on $1/T$, calculated for the same α values at the different heating rates β can be used to calculate the activation energy.

Table 1 Algebraic expression for the most frequently used mechanisms of solid state process

No	Mechanisms	Symbol	Differential form, $f(\alpha)$	Integral form, $g(\alpha)$
Sigmoidal curves				
1	N and G ($n = 1$)	A_1	$(1 - \alpha)$	$[-\ln (1 - \alpha)]$
2	N and G ($n = 1.5$)	$A_{1.5}$	$(3/2)\ (1 - \alpha)[-\ln (1 - \alpha)]^{1/3}$	$[-\ln (1 - \alpha)]^{2/3}$
3	N and G ($n = 2$)	A_2	$2\ (1 - \alpha)[-\ln (1 - \alpha)]^{1/2}$	$[-\ln (1 - \alpha)]^{1/2}$
4	N and G ($n = 3$)	A_3	$3\ (1 - \alpha)[-\ln (1 - \alpha)]^{2/3}$	$[-\ln (1 - \alpha)]^{1/3}$
5	N and G ($n = 4$)	A_4	$4\ (1 - \alpha)[-\ln (1 - \alpha)]^{3/4}$	$[-\ln (1 - \alpha)]^{1/4}$
Deceleration curves				
6	Diffusion, 1D	D_1	$1/(2\alpha)$	α^2
7	Diffusion, 2D	D_2	$1/(\ln (1 - \alpha))$	$(1 - \alpha)\ln (1 - \alpha) + \alpha$
8	Diffusion, 3D	D_3	$1.5/[(1 - \alpha)^{-1/3} - 1]$	$(1 - 2\alpha/3) - (1 - \alpha)^{2/3}$
9	Diffusion, 3D	D_4	$[1.5\ (1 - \alpha)^{2/3}][1 - (1 - \alpha)^{1/3}]^{-1}$	$[1 - (1 - \alpha)^{1/3}]^2$
10	Diffusion, 3D	D_5	$(3/2)\ (1 + \alpha)^{2/3}[(1 + \alpha)^{1/3} - 1]^{-1}$	$[(1 + \alpha)^{1/3} - 1]^2$
11	Diffusion, 3D	D_6	$(3/2)\ (1 - \alpha)^{4/3}[[1/(1 - \alpha)^{1/3}] - 1]^{-1}$	$[[1/(1 - \alpha)]^{1/3} - 1]^2$
12	Contracted geometry shape (cylindrical symmetry)	R_2	$3\ (1 - \alpha)^{2/3}$	$1 - (1 - \alpha)^{1/3}$
13	Contracted geometry shape (sphere symmetry)	R_3	$3\ (1 - \alpha)^{2/3}$	$1 - (1 - \alpha)^{1/3}$
Acceleration curves				
14	Mample power law	P_1	1	α
15	Mample power law ($n = 2$)	P_2	$2\alpha^{1/2}$	$\alpha^{1/2}$
16	Mample power law ($n = 3$)	P_3	$(1.5)\alpha^{2/3}$	$\alpha^{1/3}$
17	Mample power law ($n = 4$)	P_4	$4\alpha^{3/4}$	$\alpha^{1/4}$
18	Mample power law ($n = 2/3$)	$P_{3/2}$	$2/3(\alpha)^{-1/2}$	$\alpha^{3/2}$
19	Mample power law ($n = 3/2$)	$P_{2/3}$	$3/2(\alpha)^{1/3}$	$\alpha^{2/3}$
20	Mample power law ($n = 4/3$)	$P_{3/4}$	$4/3(\alpha)^{-1/3}$	$\alpha^{3/4}$

Invariant kinetic parameter (IKP) method [23]

The explicit temperature dependence of the rate constant is introduced by replacing $k = A\ \exp(-E/RT)$ with the Arrhenius law, which gives

$$\frac{d\alpha}{dt} = A \exp\left(\frac{-E}{RT}\right) f(\alpha) \tag{8}$$

where A is the pre-exponential factor (s^{-1}), E is the activation energy (J mol^{-1}), and R is the gas constant (J mol^{-1} K^{-1}). When the reaction is carried out by controlling

the temperature ($T = T_{0+}\beta t$, where β is the linear heating rate and T_0 the starting temperature) Eq. 8 may be written as

$$\frac{d\alpha}{dT} = \frac{A}{\beta}\exp\left(\frac{-E}{RT}\right)f(\alpha). \tag{9}$$

The thermal decomposition of a solid in an heterogeneous process is accompanied by the release of gaseous products can usually be characterized by several forms of the function $f(\alpha)$ given in Table 1. The IKP method is based on the relation of the compensation effect which described by the values of activation energies, E, and pre-exponential factors A, obtained from various conversion function using one of different methods (differential or integral methods etc.) for TG curves. To apply this method, $\alpha = \alpha(T)$ curves for several heating rates (β_v, $v = 1, 2, 3,\ldots$) are recorded and the activation parameters E and pre-exponential factors A for a set of conversion function ($f_j(\alpha)$, $j = 1, 2, 3,\ldots$), at each heating rates are calculated using an integral, differential method and other method. In this work, the CR method was used to integrate Eq. 9. It leads to the following relations:

$$\ln\frac{g_j(\alpha_{iv})}{T_{iv}^2} \cong \ln\frac{A_{jv}R}{\beta_v E_{jv}} - \frac{E_{jv}}{RT_{iv}} \tag{10}$$

with $g_j(\alpha) = \int_0^{\alpha}\frac{d\alpha}{f_j(\alpha)}$ where i is data point; β, v are the heating rate and its numbers; j is the numbers of the conversion function between 1 and 20. A plot $\ln\left[\frac{g_j(\alpha_{iv})}{T_{iv}^2}\right]$ versus $\frac{1}{T_{iv}}$ for a given analytical form of g(α) should be a straight line. We use the 20 different conversion functions given in Table 1 for the differential $f(\alpha)$ and integral $g(\alpha)$ functions in Eq. 10. 20 couples (E_{jv}, A_{jv}) of PDHBP per heating rate, β are obtained by using the CR method. The application of the IKP method is based on the study of the compensation effect. If a compensation effect is observed, a linear relation defined by Eq. 11 for each heating rate, β is obtained. It is shown by plotting ln A versus E that a compensation effect is observed for each heating rate. Thus, using the relation of the compensation effect, for each heating rate the compensation parameters (α^*, β^*) are determined.

$$\ln A = \alpha^* + \beta^* E \tag{11}$$

which leads to the *super correlation* relation.

$$\alpha^* = \ln A_{\text{int}} - \beta^* E_{\text{int}} \tag{12}$$

where α^* and β^* are constants (the compensation effect parameters). A plot α^* versus β^* is actually a straight line whose parameters allow evaluation of the invariant activation parameters. Thus, the values of invariant activation energies and invariant pre-exponential factors can be calculated from the slopes and intercepts of curves.

Determination of the kinetic model by master plots

Using a reference at point α = 0.5 and according to Eq. 2, one gets

$$g(\alpha) = \left(\frac{AE}{\beta R}\right)p(u_{0.5}) \tag{13}$$

where $u_{0.5} = E/RT$. When Eq. 2 is divided by Eq. 13, the following equation is obtained

$$\frac{g(\alpha)}{g(0.5)} = \frac{p(u)}{p(u_{0.5})}. \tag{14}$$

Plots of $g(\alpha)/g(0.5)$ against α correspond to theoretical master plots of various $g(\alpha)$ functions [24, 25]. To draw the experimental master plots of $P(u)/P(u_{0.5})$ against α from experimental data obtained under different heating rates, an approximate formula [26] of $P(u)$ with high accuracy is used $P(u) = \exp(-u)/[u(1.00198882u + 1.87391198)]$. Equation 14 indicates that, for a given α, the experimental value of $g(\alpha)/g(\alpha_{0.5})$ are equivalent when an appropriate kinetic model is used. Comparing the experimental master plots with theoretical ones can conclude the kinetic model [27].

Determination of the kinetic model by Criado–Malek–Ortega method [28]

If the value of the activation energy is known, the kinetic model of the process can be determined by this method. Criado et al. define the function

$$z(\alpha) = \frac{(d\alpha/dt)}{\beta}\pi(x)T \tag{15}$$

where $x = E/RT$, and $\pi(x)$ is an approximation of the temperature integral which cannot be expressed in a simple analytical form. In this case, the fourth rational expression of Senum and Young [29] has been used. Combining a general rate expression, $\frac{d\alpha}{dt} = kf(\alpha)$ and Eq. 15, we can obtain:

$$z(\alpha) = f(\alpha)F(\alpha). \tag{16}$$

Then the master curves of different models listed in Table 1 can be obtained following this function. Comparing the plots of $z(\alpha)$ calculated by Eq. 15 using experimental data with the master curves, the mechanism of a solid state process can be determined.

Results and discussion

According to the SEC analysis, the number-average molecular weight (M_n), weight-average molecular weight (M_w) and PDI values of PDHBP were found to be 37,500, 90,000 g mol^{-1} and 2.4 using catalysis, respectively.

Thermal decomposition process

The thermal decomposition of PDHBP was selected for the kinetic study. The activation energy of the decomposition process was determined by multiple heating rate kinetics. The typical dynamic TG thermograms of PDHBP in a dynamic nitrogen atmosphere were shown in Fig. 1, where the TG curves for the decomposition of 8–10 mg PDHBP sample were shown with 5, 10, 15 and

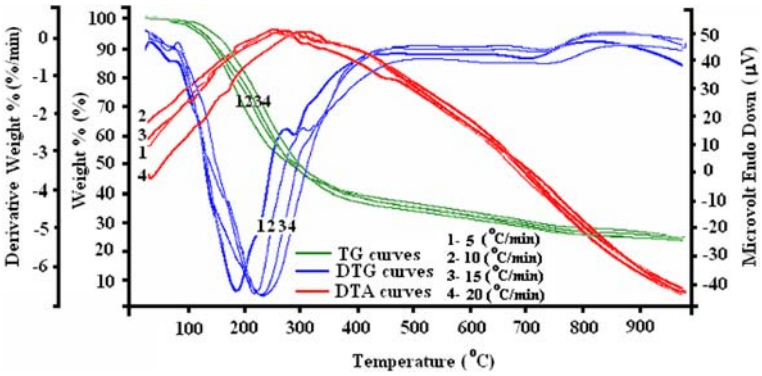

Fig. 1 TG-DTG-DTA curves of PDHBP

20 °C min^{-1} under 60 mL min^{-1} nitrogen gas. All TG curves of PDHBP showed that the thermal decomposition took place mainly in one stage and the curves shifted to the right-hand side with the temperature.

Determination of activation energy E, kinetic model $g(\alpha)$, and pre-exponential factor A

Several techniques using different approaches have been developed for solving the integral of Eq. 2. The five methods investigated in this work were those of FWO, KAS, Tang, CR and IKP method. CR method was based on a single heating rate, while the other methods were based on multiple heating rates. Isoconversional methods were firstly employed to analysis the TG data of PDHBP, because it is independent of any thermodegradation mechanisms. Equation 6 used to obtain the activation energy which can be calculated from the plot of ln $(\beta/T^{1.894661})$ versus 1,000/T and fitting to a straight line. The mean value of activation energy of thermal degradation of PDHBP in N_2 was 109.17 kJ mol^{-1}. The calculated results were summarized in Table 2.

Another isoconversion method used in this paper was that of KAS. Equation 7 utilized to determine the values of activation energy from plots of ln (β/T^2) against 1,000/T over a wide range of conversation. In this case $\alpha = 0.05, 0.1, 0.2, 0.3, 0.4, 0.5, 0.6, 0.7, 0.8, 0.9, 0.95$ were chosen to evaluate E values of PDHBP. The determined activation energies were listed in Table 2 and the average value was 109.06 kJ mol^{-1} over the range of α given. This result agrees better with the mean value of activation energy obtained by Tang method.

FWO method is an integral method also being independent of the degradation mechanism. Equation 4 has been used and the apparent activation energy of PDHBP can therefore be obtained from a plot of log β against 1,000/T for a fixed degree of conversion since the slope of such a line given by $-0.456E/RT$. Figure 2 illustrated the plots of ln β versus 1,000/T at varying conversion. The activation energies

Table 2 Activation energies and correlation coefficient of PDHBP obtained by KAS, FWO and Tang methods

Conversion	KAS method		Tang method		FWO method	
	Activation energy, E (kJ mol^{-1})	Correlation coefficient, r	Activation energy, E (kJ mol^{-1})	Correlation coefficient, r	Activation energy, E (kJ mol^{-1})	Correlation coefficient, r
0.05	92.78	0.99652	92.45	0.99230	94.29	0.99443
0.1	105.0	0.99113	104.5	0.99453	108.4	0.99125
0.2	106.4	0.99561	113.4	0.99175	113.9	0.99613
0.3	106.0	0.99766	105.5	0.99897	107.7	0.99621
0.4	108.1	0.99757	107.7	0.99211	109.9	0.99725
0.5	105.0	0.99811	102.9	0.99972	105.5	0.99621
0.6	107.0	0.99223	106.5	0.99249	109.4	0.99238
0.7	106.6	0.99310	106.2	0.99614	109.2	0.99614
0.8	108.4	0.99121	107.9	0.99512	111.2	0.99212
0.9	130.3	0.98905	128.2	0.98991	130.7	0.98173
0.95	124.4	0.98911	123.8	0.98731	127.2	0.98724
Mean	109.1		109.0		110.0	

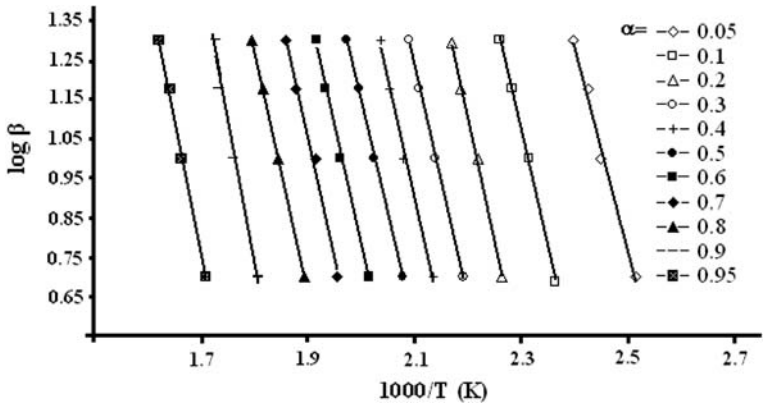

Fig. 2 FWO plots of PDHBP at varying conversation in N_2

calculated from the slopes were tabulated in Table 2 and the mean value of activation energy was 110.06 kJ mol^{-1}. Comparatively, the E value of PDHBP was very close to ones obtained by the two methods. The E values of PDHBP obtained by Tang, KAS and FWO methods were 109.17, 109.06 and 110.06 kJ mol^{-1}, respectively.

Constant mass loss lines were determined by measuring the temperature at a given mass percent for each rate. In Fig. 3 the Arrhenius type plots of dynamic TG runs were shown for mass ranging from $\alpha = 0.05$ to 0.95 in N_2. Table 2 summaries the activation energy and correlation coefficient on the overall mass loss from 5 to

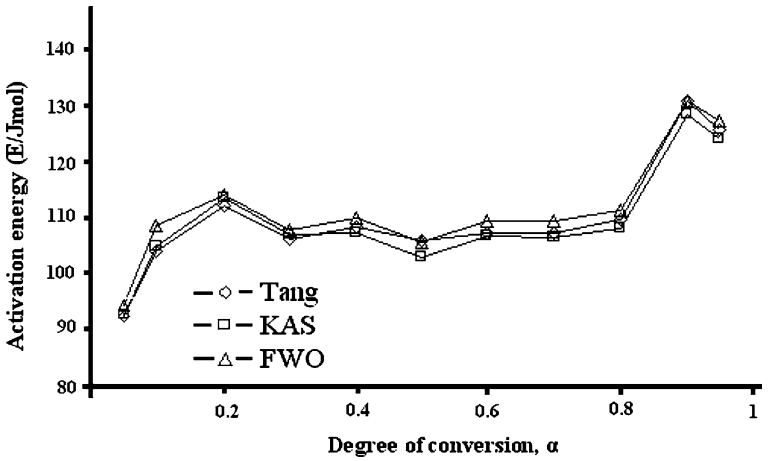

Fig. 3 Activation energy (E) as a function of degree of conversion for the decomposition process of PDHBP calculated by Tang, KAS and FWO methods

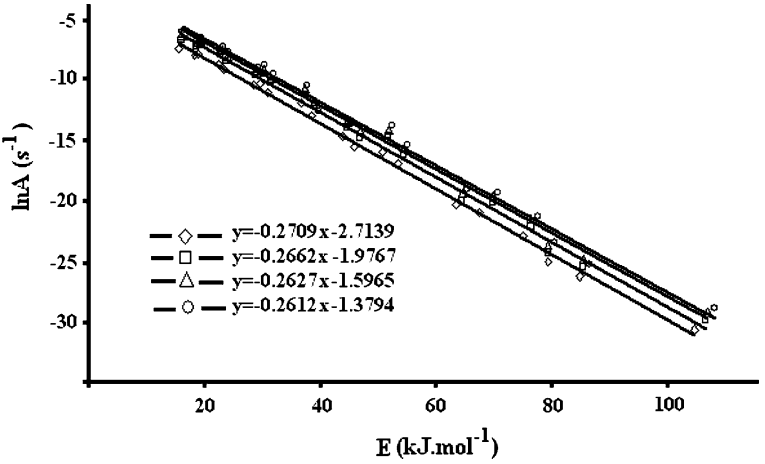

Fig. 4 Compensation effect for PDHBP versus heating rates

95 mass % in N_2. The results indicated an acceptable correlation coefficient always superior to 0.98173.

The thermal decomposition of PDHBP in N_2 presented a same behavior for Tang, KAS and FWO method. The initial activation energy required to initial decomposition was about 93 kJ mol^{-1}. When 90% mass of PDHBP was loss the activation energy increased to a maximum value of about 130 kJ mol^{-1}.

Other method using the calculation of kinetic parameters is IKP. The application of the IKP method is based on the study of the compensation effect. If a compensation effect is observed, a linear relation defined by Eq. 5 for each heating

Table 3 The values of α^* and β^* for PDHBP versus heating rates

β/°C min^{-1}	α^*	β^*	r
5	−0.2709	−2.7139	0.99905
10	−0.2662	−1.9767	0.99810
15	−0.2627	−1.5967	0.99840
20	−0.2612	−1.3794	0.99995

rate, β is obtained. It is shown by plotting ln A versus E that a compensation effect is observed for each heating rate (Fig. 4).

Thus, using the relation of the compensation effect, for each heating rate the compensation parameters (α^*, β^*) are determined.

$$\ln A = \alpha^* + \beta^* E \tag{17}$$

which leads to the *super correlation* relation.

$$\alpha^* = \ln A_{\text{int}} - \beta^* E_{\text{int}} \tag{18}$$

where α^* and β^* are constants (the compensation effect parameters).

The values of α^* and β^* obtained for PDHBP are presented in Table 3. Thus, the values of invariant activation energies and invariant pre-exponential factors can be calculated from the slopes and intercepts of curves.

A plot α^* versus β^* is actually a straight line whose parameters allow evaluation of the invariant activation parameters (Fig. 5).

The significance of α^* and β^* being characteristics of the experimental conditions has been demonstrated by Lesnikovich and Levchik [30]. Consequently, the values of the invariant activation energy and the invariant pre-exponential factor calculated from the slope and intercept of the straight line obtained by using Eq. 6 is found to be 109.82 kJ mol^{-1} and 27.28. The regression coefficient of this curve is 0.99970.

In order to find out the mechanism of the thermal decomposition of PDHBP, CR method has been chosen as it involves the mechanisms of solid-state process.

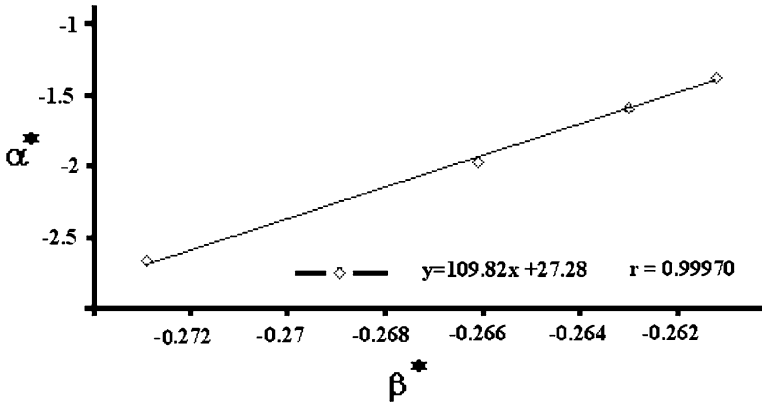

Fig. 5 Verifying super correlation relation (Eq. 6)

Table 4 Activation energies and preexponential factors of PDHBP obtained by CR method in N_2 atmosphere

	5 °C min^{-1}			10 °C min^{-1}			15 °C min^{-1}			20 °C min^{-1}		
	E (kJ mol^{-1})	ln A	r	E (kJ mol^{-1})	ln A	r	E (kJ mol^{-1})	ln A	r	E (kJ mol^{-1})	ln A	r
A_1	50.83	−15.35	0.98212	51.84	−14.62	0.98521	51.93	−14.09	0.98422	52.58	−13.84	0.98421
$A_{1.5}$	36.54	−11.90	0.98533	37.28	−11.21	0.98432	37.37	−10.72	0.98354	37.84	−10.46	0.98482
A_2	29.39	−10.24	0.98476	30.01	−9.544	0.97978	30.14	−9.094	0.97927	30.45	−8.821	0.98247
A_3	22.25	−8.631	0.98223	22.73	−7.946	0.98313	22.82	−7.516	0.98123	23.16	−7.242	0.98112
A_4	18.62	−7.862	0.99314	19.09	−7.181	0.99214	19.18	−6.762	0.99243	19.41	−6.494	0.99533
D_1	68.78	−20.97	0.98741	70.16	−20.22	0.98623	70.11	−19.60	0.98461	71.06	−19.38	0.98634
D_2	75.21	−22.95	0.99242	76.69	−22.18	0.99127	76.67	−21.54	0.98973	77.73	−21.33	0.98785
D_3	78.04	−25.03	0.99521	79.59	−24.26	0.99431	79.58	−23.61	0.99286	80.69	−23.40	0.99213
D_4	83.97	−26.23	0.99465	85.61	−25.46	0.99321	85.62	−24.80	0.99523	86.73	−26.89	0.99164
D_5	63.53	−22.20	0.99511	64.78	−21.45	0.99233	64.72	−20.84	0.99431	65.61	−20.61	0.98956
D_6	105.0	−30.62	0.99822	107.0	−29.81	0.99811	107.1	−29.11	0.99761	108.4	−28.90	0.99843
R_2	43.81	−14.66	0.98832	44.69	−13.94	0.98897	44.74	−13.43	0.98823	45.32	−13.65	0.98823
R_3	45.95	−15.49	0.98113	46.88	−14.76	0.98865	46.94	−14.24	0.98864	47.55	−14.00	0.98855
P_1	38.37	−12.93	0.96636	39.16	−12.23	0.96811	39.19	−11.72	0.97124	39.71	−13.79	0.98521
P_2	23.17	−9.131	0.98533	23.67	−8.447	0.98925	23.73	−7.991	0.97991	24.03	−7.735	0.98373
P_3	18.12	−7.933	0.98412	18.53	−7.265	0.98432	18.57	−6.834	0.97931	18.81	−6.566	0.97924
P_4	15.56	−7.374	0.98451	15.92	−6.692	0.98631	16.00	−6.285	0.98342	16.19	−6.017	0.98501
$P_{3/2}$	53.57	−16.91	0.98542	54.66	−16.18	0.98543	54.65	−15.62	0.98635	55.39	−15.39	0.97912
$P_{2/3}$	28.23	−10.37	0.98822	28.83	−9.671	0.98844	28.88	−9.216	0.98847	29.26	−8.964	0.98839
$P_{3/4}$	30.77	−11.00	0.97211	31.42	−10.30	0.97813	31.46	−9.838	0.97542	31.87	−9.572	0.97772

According to Eq. 5, activation energy for every $g(\alpha)$ function listed in Table 1 can be calculated at constant heating rates from fitting of ln $(g(\alpha)/T^2)$ versus 1,000/T plots. The activation energies and the correlations at constant heating rates such as 5, 10, 15 and 20 °C min^{-1} were tabulated in Table 4 for thermal degradation of PDHBP. In order to determine the mechanism the degradation of PDHBP agreed better with, we have compared the activation energies obtained by methods above. According to Table 4, it was could be found that the E values of PDHBP in N_2 corresponding to mechanism D_6 had best agreement with the values obtain d by Tang, KAS and FWO methods.

Especially at the heating rate in 20 °C min^{-1}, the activation energy corresponding to mechanism D_6 is 108.4 kJ mol^{-1}, which was very close to the value of 109.17 kJ mol^{-1} obtained by Tang method. The correlation coefficient was also much higher than other. In order to confirm the conclusions, the experimental master plots $P(u)/P(u_{0.5})$ against α constructed from experimental data of the thermal decomposition of PDHBP under different heating rates and the theoretical master plots of various kinetic functions were all shown in Fig. 6. The comparisons of the experimental master plots with theoretical ones indicated that the kinetic process of the thermal decomposition of PDHBP agreed with the D_6 master curve very well.

By assuming D_n law, experimental data, the expression of the D_n model, and the average reaction energy predetermined were introduced into Eq. 2, the following expression was obtained.

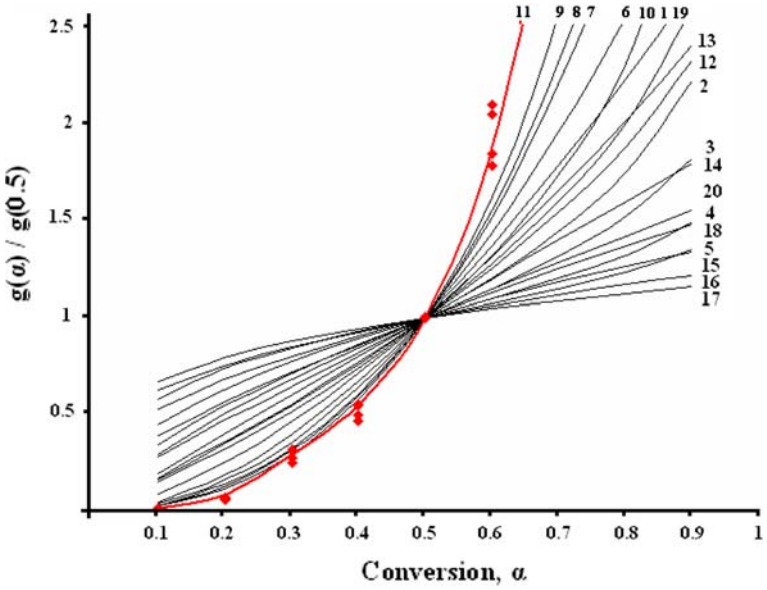

Fig. 6 Master plots of theoretical $g(\alpha)/g(0.5)$ against α for various reaction models (*solid curves* represent 20 kinds of reaction models given in Table 1) and experimental data (*dark filled triangle*) of PDHBP at the heating rates 5, 10, 15 and 20 °C min^{-1}

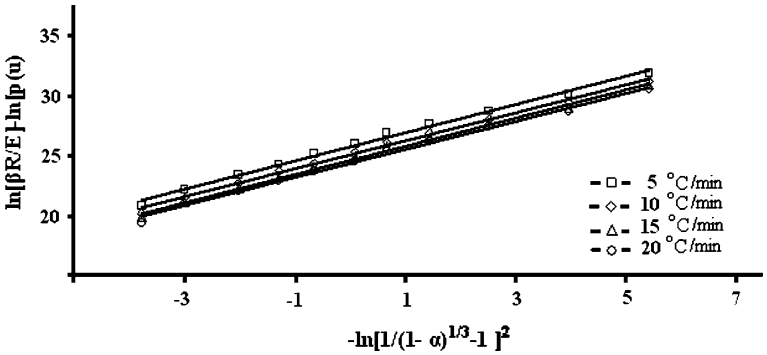

Fig. 7 Plotting ln $[\beta R/E] - \ln [P(u)]$ against $-\ln [[1/(1-\alpha)]^{1/3} - 1]^2$ for PDHBP at heating rates

Table 5 Preexponential factors and correlation coefficients obtained by plotting $\ln [\beta R/E] - \ln [P(u)]$ against $-\ln [[1/(1-\alpha)]^{1/3} - 1]^2$

β (K mol^{-1})	ln A (s^{-1})	r
5	25.67	0.99562
10	25.06	0.99863
15	24.66	0.99876
20	24.38	0.99768
Mean	24.94	

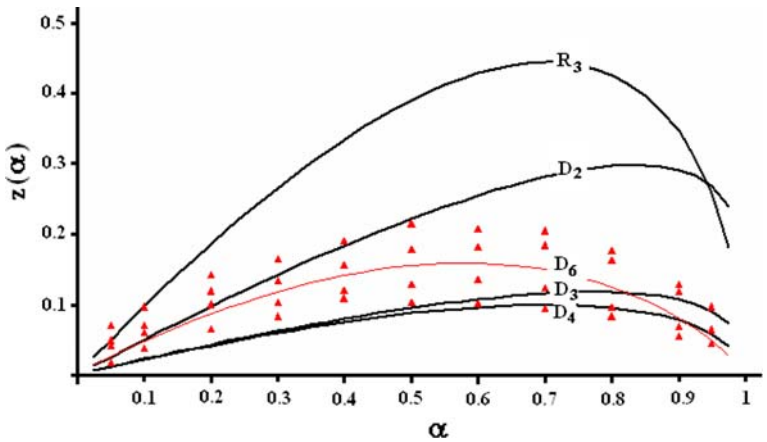

Fig. 8 Master curves of $z(\alpha)$ and experimental data

$$\ln [\beta R/E] - \ln [P(u)] = \ln A - \ln [[1/(1-\alpha)]^{1/3} - 1]^2 \quad (19)$$

A group of lines were obtained by plotting ln $[\beta R/E]$ – ln $[P(u)]$ against –ln $[[1/(1-\alpha)]^{1/3} - 1]^2$. As shown in Fig. 7 and Table 5, the pre-exponential factor was calculated from the intercepts of the lines corresponding to various heating rates.

Also, we have employed reference theoretical master curves too, in order to find out the reaction mechanism for PDHBP. According to the Criado et al., a master plot is a characteristic curve independent of the condition of the measurement. The master curve plots of $z(\alpha)$ versus α for different mechanisms have been illustrated in Fig. 8.

The experimental data of $z(\alpha)$ for PDHBP agree very well with the deceleration D_6 master curve. This result had best agreement with the mechanisms type obtained by Master plot methods.

Consequently, Poly(2,2′-dihydroxybiphenyl) was synthesized by oxidative polymerization process. The activation energies for thermal degradation of PDHBP in N_2 obtained by Tang, KAS, FWO, CR and IKP methods were 109.1, 109.0, 110.0, 108.4 and 109.8 kJ mol^{-1}, respectively. The resulting logarithmic values of the pre-exponential factor ln A (s^{-1}) obtained from master plots method and IKP method was 24.94 and 27.28. Thermal degradation mechanism for PDHBP according to the analysis of the results obtained by CR method, master plots method and Criado–Malek–Ortega method is a decelerated D_n type, which indicates a solid-state process based on an n-dimensional diffusion.

Conclusion

PDHBP was synthesized by catalytic oxidative polymerization using a catalysis. The M_n, M_w and PDI values of PDHBP were found to be 37,500, 90,000 g mol^{-1} and 2.4, respectively. The kinetic of the thermal degradation of PDHBP was investigated by thermogravimetric analysis at different heating rates. The apparent activation energies of thermal decomposition for PDHBP as determined by isoconversional methods such as Tang, FWO, KAS, CR and IKP were 109.1, 109.0, 110.0, 108.4 and 109.8 kJ mol^{-1}, respectively. The most likely decomposition process was a D_n Deceleration type in terms of the Coats–Redfern, master plots and Criado–Malek–Ortega results. The logarithmic values of the pre-exponential factor ln A obtained from master plots method and IKP method was 24.94 and 27.28.

References

1. Xu MH, Lin ZM, Pu L (2001) Construction of an *ortho*-phenol polymer. Tetrahedron Lett 42(36):6235–6238
2. Higashimura H, Kubota M, Shiga A, Kodera M, Uyama H, Kobayashi S (2000) "Radical-controlled" oxidative polymerization of 4-phenoxyphenol catalyzed by a dicopper complex of a dinucleating ligand. J Mol Catal A Chem 161:233–237
3. Kurisawa M, Chung JE, Uyama H, Kobayashi S (2003) Thermo- and pH-responsive biodegradable poly(alpha-*N*-substituted gamma-glutamine)s. Biomacromolecules 4:1394–1399
4. Kobayashi S, Higashimura H (2003) Oxidative polymerization of phenols revisited. Prog Polym Sci 28:1015–1048
5. Ikeda R, Maruichi N, Tonami H, Tanaka H, Uyama H, Kobayashi S (2000) Peroxidase-catalyzed polymerization of fluorine-containing phenols. J Macromol Sci Pure Appl Chem 37(9):983–995
6. Tonami H, Uyama H, Kobayashi S, Fujita T, Taguchi Y, Osada K (2000) Chemoselective oxidative polymerization of *m*-ethynylphenol by peroxidase catalyst to a new reactive polyphenol. Biomacromolecules 1(2):149–151

7. Kobayashi S, Uyama H, Kimura S (2001) Enzymatic polymerization. Chem Rev 101(12):3793–3818
8. Tonami H, Uyama H, Oguchi T, Higashimura H, Kobayashi S (1999) Synthesis of a soluble polyphenol by oxidative polymerization of bisphenol-A using iron-salen complex as catalyst. Polym Bull 42(2):125–129
9. Saito K, Sun G, Nishide H (2007) Green synthesis of soluble polyphenol: oxidative polymerization of phenol in water. Green Chem Lett Rev 1(1):47–51
10. Uyama H, Maruichi N, Tonami H, Kobayashi S (2002) Peroxidase-catalyzed oxidative polymerization of bisphenols. Biomacromolecules 3(1):187–193
11. Oguchi T, Tawaki S, Uyama H, Kobayashi S (1999) Soluble polyphenol. Macromol Rapid Commun 20(7):401–403
12. Bilici A, Kaya İ, Doğan F (2009) Monomer/polymer Schiff base copper (II) complexes for catalytic oxidative polymerization of 2,2′-dihydroxybiphenyl. J Polym Sci Part A Polym Chem (accepted)
13. Demir HÖ, Kaya İ, Saçak M (2008) The oxidative polycondensation of 2-[(4-pyridilmethylene)-imino]phenol by molecular O-2 in alkaline medium: synthesis and characterization. Polym Bull 60(1):37–48
14. Demir HÖ (2006) Polymerization of pyridilazomethinphenols. PhD Thesis, Ankara University, Ankara, Turkey
15. Flynn J, Wall L (1966) A quick, direct method for the determination of activation energy from thermogravimetric data. Polym Lett 4(5):323–328
16. Ozawa T (1965) A new method of analyzing thermogravimetric data. Bull Chem Soc Jpn 38: 1881–1888
17. Doyle CJ (1961) Synthesis and evaluation of thermally stable polymers. II. Polymer evaluation. Appl Polym Sci 5:285–292
18. Coats A, Redfern J (1964) Kinetics parameters from thermogravimetric data. Nature 201:68–69
19. Criado J, Malek J, Ortega A (1989) Applicability of the master plots in kinetic analysis of non-isothermal data. Thermochim Acta 147(2):377–385
20. Nunez L, Fraga F, Villanueva M (2000) Thermogravimetric study of the decomposition process of the system BADGE (*n*=0)/1,2 DCH. Polymer 41:4635–4641
21. Tang W, Liu Y, Zhang CH, Wang C (2003) New approximate formula for Arrhenius temperature integral. Thermochim Acta 408(1–2):39–43
22. Kissinger HE (1957) Reaction kinetics in different thermal analysis. Anal Chem 29(11):1702–1709
23. Levchik SV, Levchik GF, Lesnikovich AL (1985) Analysis and development of effective invariant kinetic-parameters finding method based on the non-isothermal data. Thermochim Acta 92:157–160
24. Gotor FJ, Criado JM, Malek J, Koga N (2000) Kinetic analysis of solid-state reactions: the universality of master plots for analyzing isothermal and nonisothermal experiments. J Phys Chem A 104(46):10777–10782
25. Perez-Maqueda LA, Criado JM, Gotor FJ, Malek J (2002) Advantages of combined kinetic analysis of experimental data obtained under any heating profile. J Phys Chem A 106(12):2862–2868
26. Wanjun T, Yuwen L, Hen Z, Zhiyong W, Cunxin W (2003) New temperature integral approximate formula for non-isothermal kinetic analysis. J Therm Anal Cal 74(1):309–315
27. Wanjun T, Yuwen L, Xi Y, Cunxin W (2004) Kinetic studies of the calcination of ammonium metavanadate by thermal methods. Ind Eng Chem Res 43(9):2054–2059
28. Criado JM, Malek J, Ortega A (1989) Applicability of the master plots in kinetic-analysis of non-isothermal data. Thermochim Acta 147(2):377–385
29. Senum GI, Yang KT (1977) Rational approximations of the integral of the Arrhenius function. J Therm Anal 11(13):445–447
30. Lesnikovich AL, Levchik SV (1985) Invariant kinetic-parameters of polybutadiene binders thermal-decomposition. J Propul Power 1(4):311–312